

Processing of Human Toll-like Receptor 7 by Furin-like Proprotein Convertases Is Required for Its Accumulation and Activity in Endosomes

Madeleine M. Hipp,¹ Dawn Shepherd,¹ Uzi Gileadi,¹ Michael C. Aichinger,¹ Benedikt M. Kessler,² Mariola J. Edelmann,² Rachid Essalmani,³ Nabil G. Seidah,³ Caetano Reis e Sousa,^{4,5,*} and Vincenzo Cerundolo^{1,5,*}

¹MRC Human Immunology Unit, Weatherall Institute of Molecular Medicine, University of Oxford, Oxford OX3 9DU, UK

²Henry Wellcome Building for Molecular Physiology, Nuffield Department of Medicine, Centre for Cellular and Molecular Physiology, Churchill Hospital, Oxford OX3 7BN, UK

³Institut de Recherches Cliniques de Montréal (IRCM), affiliated to the University of Montreal, Montréal, Québec H2W 1R7, Canada

⁴Immunobiology Laboratory, Cancer Research UK, London Research Institute, London WC2A 3LY, UK

⁵These authors contributed equally to this work

*Correspondence: caetano@cancer.org.uk (C.R.e.S.), vincenzo.cerundolo@imm.ox.ac.uk (V.C.)

<http://dx.doi.org/10.1016/j.immuni.2013.09.004>

SUMMARY

Toll-like receptor 7 (TLR7) triggers antiviral immune responses by recognizing viral single-stranded RNA in endosomes, but the biosynthetic pathway of human TLR7 (hTLR7) remains unclear. Here, we show that hTLR7 is proteolytically processed and that the C-terminal fragment selectively accumulates in endocytic compartments. hTLR7 processing occurred at neutral pH and was dependent on furin-like proprotein convertases (PCs). Furthermore, TLR7 processing was required for its functional response to TLR7 agonists such as R837 or influenza virus. Notably, proinflammatory and differentiation stimuli increased the expression of furin-like PCs in immune cells, suggesting a positive feedback mechanism for TLR7 processing during infection. Because self-RNA can under certain conditions activate TLR7 and trigger autoimmunity, our results identify furin-like PCs as a possible target to attenuate TLR7-dependent autoimmunity and other immune pathologies.

INTRODUCTION

Toll-like receptors (TLRs) have emerged as major regulators of innate and adaptive immune responses to infection. Many TLRs recognize products of microbial biosynthesis pathways, which are absent in mammals, allowing for qualitative discrimination between microbial and host cells (Akira et al., 2006). In contrast, TLR7 and TLR8 respond to viral and bacterial single-stranded (ss) RNA and TLR9 to DNA which, barring small differences, are effectively invariant between host and pathogen. This raises the issue of how TLRs 7, 8, and 9 can successfully discriminate self from nonself. The nucleic acid-recognizing TLRs do not respond to their ligands at the cell surface but in endosomes (Blasius and Beutler, 2010; Kagan, 2012). This has led to the notion that discrimination is achieved on the basis of ligand local-

ization and that responses to self nucleic acids are avoided in part through the absence of the latter from endosomal compartments (Blasius and Beutler, 2010; Kagan, 2012). Consistent with that notion, TLR7 and TLR9 can respond to self-RNA or -DNA, respectively, if the latter are deliberately introduced into the endocytic pathway (Diebold et al., 2004, 2006; Heil et al., 2004; Leadbetter et al., 2002). This process may occur naturally in some instances and contribute to autoimmunity in genetically susceptible individuals (Krug, 2008; Shlomchik, 2009).

Newly synthesized TLR7, TLR8, and TLR9 translocate into the endoplasmic reticulum (ER), from which they traffic to endosomes with help of the associated protein Unc93B1 (Brinkmann et al., 2007; Kim et al., 2008; Lee et al., 2013). A possible explanation as to why nucleic acid-recognizing TLRs respond to their ligands only within endosomal compartments has come from the observation that they undergo proteolytic cleavage in endosomes and that this cleavage is necessary for receptor activity (Ewald et al., 2011; Lee et al., 2013; Park et al., 2008; Sepulveda et al., 2009). Low pH-dependent endosomal cathepsins, as well as asparaginyl endopeptidase (AEP), process mouse TLR9 (mTLR9) and these proteases might constitute attractive targets for inhibition in cases of TLR-driven autoimmunity or pathological inflammation (Ewald et al., 2011; Park et al., 2008; Sepulveda et al., 2009). mTLR7 is also cleaved by AEP (Maschalidi et al., 2012). However, inhibition of cathepsins or AEP does not completely prevent mouse TLR processing (Ewald et al., 2008; Sepulveda et al., 2009), indicating involvement of additional proteases. In addition, although human TLR9 (hTLR9) has also been suggested to be cleaved by AEP (Sepulveda et al., 2009), most analysis of TLR processing has been carried out with the mouse receptors. Thus, there is a need to establish whether all TLRs are processed similarly, whether this is true for human as well as mouse receptors, and what other proteases might be involved in cleavage.

The furin-like proprotein convertases (PCs) are a family of proteases involved in processing of many polypeptides (Seidah et al., 2008), including Notch, viral glycoproteins, growth factors and their receptors, neuropeptides, metalloproteases, adhesion molecules, enzymes, and even toxins (Hallenberger et al., 1992; Logeat et al., 1998; Molloy et al., 1992; Rousselet et al., 2011b;

Zarkik et al., 1997). Furin-like PCs encompass a family of nine calcium-dependent serine endoproteases of the subtilisin-kexin type called PC1/3, PC2, Furin, PC4, PC5/6, PACE4, PC7, SKI-1/S1P, and PCSK9 (Seidah et al., 2008). The first seven enzymes cleave their substrates after the C-terminal residue at sites bearing the consensus motif matching the consensus K/R_xnK/R, where x indicates any amino acid residue, K/R designates a lysine or an arginine residue, and n is 0, 2, 4, or 6 (Seidah et al., 2008). PCs are synthesized as inactive proenzymes and the inhibitory prosegment is removed through an initial autocatalytic processing event in the ER (all but PC2) or in immature secretory granules (PC2) (Fugère et al., 2002; Seidah et al., 2008). The heterodimer complex, consisting of the inhibitory prosegment and the rest of the molecule, then traffics from the ER to specific subcellular compartments where catalytic activity is acquired, usually after a second autocatalytic cleavage of the prosegment that results in its release from the active enzyme (Seidah et al., 2008). PC1/3 and PC2 are restricted to dense core secretory granules of secretory cells whereas PC4 is found primarily in testicular and ovarian tissues. In contrast, furin, PACE4, PC5/6A, PC5/6B, and PC7 are ubiquitously expressed in multiple cell types and located throughout the secretory pathway (Fugère et al., 2002; Seidah et al., 2008). Notably, furin-like PCs can be active at neutral pH (Decroly et al., 1996; Malfait et al., 2008; Molloy et al., 1992) and generally cleave their substrates in the trans-Golgi network (TGN), elsewhere along the secretory pathway, or at the cell surface (Rousselet et al., 2011a; Seidah et al., 2008). Rarely, cleavage can also occur in early biosynthetic compartments such as the ER in cases where the substrate outcompetes the inhibitory prosegment of the convertase (Salvas et al., 2005). Their broad expression pattern, cleavage specificity, ability to act in endosomes, and localization along the secretory pathway suggest that some furin-like PCs could potentially contribute to TLR processing.

In this study, we show that hTLR7 undergoes proteolytic processing and that the C-terminal fragment of the receptor selectively accumulates in endocytic compartments. hTLR7 processing was independent of low pH and largely independent of cathepsin activity. Instead, hTLR7 processing was dependent on the action of furin-like PCs. Our data underscore the notion that endosomal TLRs are regulated by proteolysis and indicate that this can occur at neutral pH, possibly in early endosomes or in a pre-endosomal compartment, such as the ER, Golgi, or plasma membrane. These results have implications for our understanding of self/nonself nucleic acid discrimination and highlight furin-like PCs as a possible target in attenuation of TLR7-dependent autoimmunity and other immune pathologies.

RESULTS

Processing of Human TLR7 Generates a Truncated C-Terminal Fragment that Accumulates in Phagosomes

To determine whether hTLR7 undergoes posttranslational proteolytic processing, we tagged hTLR7 with a hemagglutinin (HA) epitope at the carboxyl (C) terminus (TLR7-HA) and stably expressed it in THP-1 (THP-TLR7), HEK293null (293null-TLR7), and LoVo (LoVo-TLR7) cell lines. Immunoblot analysis with anti-HA revealed a prominent band corresponding to the expected ~150 kD polypeptide, which was absent from green fluo-

rescence protein (GFP)-expressing controls (Figure 1A). Notably, anti-HA additionally detected a fainter band at around ~75 kD in TLR7-HA-expressing cells, but not in GFP-expressing controls (Figure 1A). We confirmed that the 75 kD polypeptide corresponds to a C-terminal fragment of TLR7 by immunoprecipitation from lysates of THP-TLR7 followed by SDS-PAGE and mass spectrometry analysis of the excised band (Figure 1B). Figure 1C shows the protein sequence of hTLR7 with the peptides detected by mass spectrometry highlighted in black. All peptides mapped C-terminal of a region encompassing residues 455–493 (Figure 1C, blue). This region is thought to form a flexible loop between the leucine-rich repeats (LRR) 14 and 15 (Bell et al., 2003) and its exposure might therefore make it a suitable target for proteolytic enzymes.

Pretreatment of THP-TLR7 cells with PMA to induce differentiation into macrophage-like cells, or with proinflammatory cytokines such as IFN- γ or IFN- α , led to an increase in total detectable amount of TLR7 (Figures S1A and S1B available online and data not shown). The same treatments also increased the ratio of truncated 75 kDa to full-length 150 kDa TLR7 (Figures 2A, 2B, S1A, and S1B) and potentiated the ability of THP-TLR7 cells to produce IL-8, IL-6, and TNF- α in response to the specific TLR7 agonist R837 (Figures 2A and 2B and data not shown). Increased detection of truncated TLR7 was also seen after treatment with the TLR4 agonist LPS (Figure 2C). Similarly, pretreatment of primary human B cells with PMA, B cell receptor crosslinking \pm CD40L, IFN- α , or IFN- γ also enhanced their ability to respond to R837, as measured by cell surface staining for CD83 (Figure S1C and data not shown). Thus, exposure of cells to differentiation-inducing or proinflammatory cytokines increases the amount of truncated TLR7 in total cell lysates and/or responsiveness to TLR7 agonists.

We investigated whether truncated TLR7 might correspond to a signaling-competent form of the receptor that localizes selectively to the endocytic pathway in which ligand is encountered. Consistent with that notion, phagosome preparations isolated from R837-stimulated THP-TLR7 that had been fed latex beads contained almost exclusively truncated TLR7 (Figure 2D). This was in contrast to cell lysates, which contained the usual ratio of truncated and total receptor (Figure 2D). As expected, phagosome preparations were positive for the lysosomal protein LAMP1 but devoid of the ER marker calnexin (Figure 2D). Cleaved TLR7 was detected in phagosomes isolated as early as 15 min after latex bead incubation and cleavage was unaffected by the addition of R837 (Figures S1D and S1E). We conclude that hTLR7, like mTLR9 (Ewald et al., 2008) and mTLR7 (Maschalidi et al., 2012), undergoes N-terminal processing to generate a C-terminal fragment that selectively accumulates in endocytic compartments.

Human TLR7 Processing Is Independent of Low pH

Processing of mTLR7 and mTLR9 mediated by cathepsins of the cysteine protease family and/or AEP is strictly dependent on endosomal acidification (Ewald et al., 2008; Park et al., 2008; Sepulveda et al., 2009). We examined the effect of raising endosomal pH in THP-TLR7 cells that had been pretreated with PMA to increase generation of truncated receptor (see above). The ratio of truncated to total TLR7 in total cell lysates, as well as the appearance of truncated TLR7 in phagosomes,

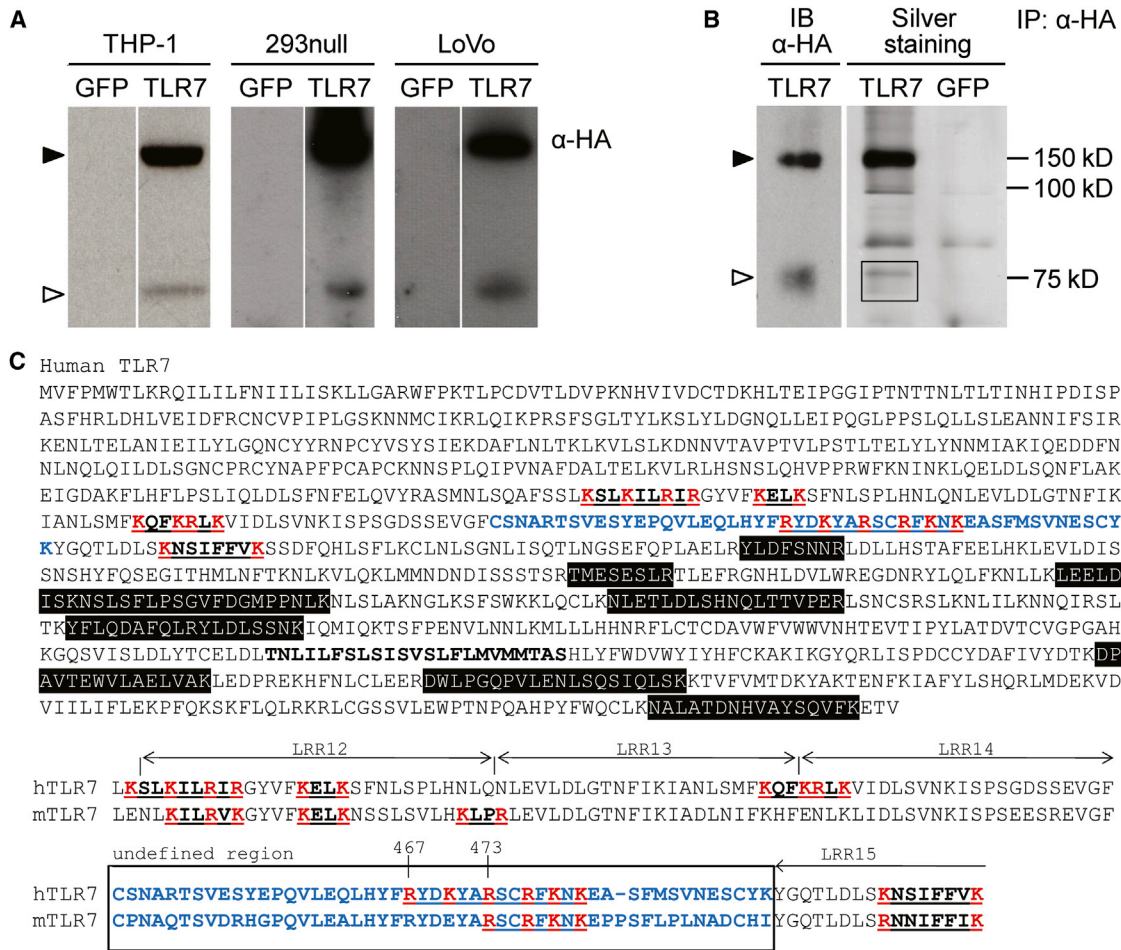


Figure 1. A Truncated C-Terminal Fragment of TLR7 Is Present in Different Human Cell Lines

(A) HA-tagged proteins from THP-, 293null-, or LoVo-TLR7 cell lysates were analyzed by immunoblot with anti-HA. Representative of more than three independent experiments. Full-length and truncated TLR7 are shown by filled and open arrowheads, respectively. (B) Comparison of immunoblot and silver staining of proteins immunoprecipitated with anti-HA from THP-TLR7 or THP-GFP treated with PMA for 24 hr. Box indicates polypeptides analyzed by nano LC-ESI/MS tandem mass spectrometry. MS analysis was performed once. (C) Top: hTLR7 sequence, with peptides identified by MS analysis highlighted in black. The undefined region predicted by Bell et al. (2003) is shown in blue. Potential furin-like PC recognition sites are underlined. Arginine and lysine residues within those sites are shown in red. Bottom: Alignment of the potential PC recognition sites close to the undefined region within the hTLR7 and mTLR7 sequences.

was unaffected by bafilomycin A, an inhibitor of the vacuolar H⁺-ATPase, or monensin, a monovalent ionophore that dissipates proton gradients (Figure 3A). As a positive control, the same drug treatments blocked the conversion of pro-cathepsin (Cat) B into mature enzyme and the trafficking of mature CatB into phagosomes, as detected by probing cell lysates and phagosomal fractions, respectively (Figure 3A). However, the block in acidification prevented IL-8 production by PMA-treated THP-TLR7 cells in response to R837 without affecting the viability of the cells or their response to LPS (Figure S2A). Furthermore, when we used the broad-range cathepsin inhibitor E64 supplemented with inhibitors specific for CatS and CatK, we did not see inhibition of either TLR7 processing or R837-elicited IL-8 production (Figures 3B and 3C). However, when we used EST, a more cell-permeable version of E64, we saw accumulation of full-length TLR7 alongside cleaved TLR7 in phagosomes (Figure 3B). Nevertheless, EST was not sufficient to decrease

the functional response of THP-TLR7 cells to R837 (Figure 3C, right). Thus, endosomal acidification and cathepsin-like activity appear largely dispensable for processing of hTLR7 in THP-1 cells.

Calcium-Dependent Serine-Proteases of the Furin-like PCs Mediate Processing of Human TLR7

To test the involvement of other proteases in TLR7 processing, PMA-differentiated THP-TLR7 were treated with a range of inhibitors. To obviate possible toxicity and to control for specificity, we first titrated all drugs to identify the maximum concentration that did not cause cell death or prevent responses to LPS (Figure S2B and data not shown). The serine-protease inhibitor AEBSEF reduced the detection of truncated TLR7 in cell lysates and decreased the response of THP-TLR7 to R837 but not to LPS when compared to the DMSO control (Figure 4A). Similar results were obtained with a second serine protease inhibitor,

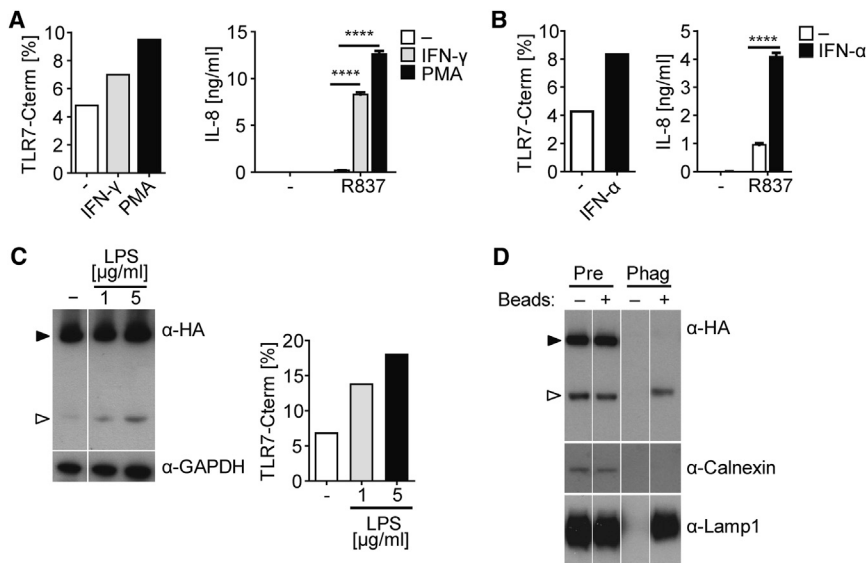


Figure 2. Proinflammatory Stimuli Enhance TLR7 Processing and Responses to TLR7 Agonists

(A–C) Immunoblot analysis of cell lysates from THP-TLR7 treated for 24 hr with 10 nM PMA, 200 U/ml IFN- γ (A), 1,000 U/ml IFN- α (B), or LPS (C). Intensity of truncated TLR7 band is expressed as percentage of the truncated + full-length TLR7 bands. (A and B) THP-TLR7 were differentiated with PMA, IFN- γ , or IFN- α as above and then stimulated with R837 for another 24 hr. Values are mean \pm SD of triplicates. **** p < 0.0001 versus control by Student's t test.

(D) Phagosomes were isolated from THP-TLR7 fed with or without latex beads in the presence of R837. Lysates of pregradient (Pre) controls or phagosome (Phag) were analyzed by immunoblot. Full-length and truncated TLR7 are shown by filled and open arrowheads, respectively. Representative of at least three independent experiments. See also Figure S1.

TPCK (data not shown). In addition, calcium depletion via EDTA in combination with the calcium ionophore A23187 also reduced cleavage of TLR7 and selectively impaired the response of THP-TLR7 to R837 but not to LPS (Figure 4B). Taken together, these results suggested the involvement of a calcium-dependent serine protease in hTLR7 processing.

THP-1 cells contained mRNA for *Furin*, *Pc1/3* (*Pcsk1*), *Pace4*, *Pc5/6* (*Pcsk5/6*), and *Pc7* (*Pcsk7*), especially after PMA-induced differentiation or treatment with proinflammatory cytokines (Figure S3A and data not shown). We confirmed by immunoblot that PMA, LPS, and IFN- γ induce the upregulation of furin protein in THP-1 cells (Figure S3B). Therefore, we tested whether TLR7 processing in PMA-treated THP-TLR7 cells was affected by DC1, a dicoumarol derivative that potently inhibits furin, PACE4, PC5/6, and (to a lesser extent) PC7 (Komiyama et al., 2009). Notably, DC1 treatment reduced the ratio of truncated to total TLR7 in total lysates of THP-TLR7 cells, which correlated with a decrease in the response to R837 but not to LPS (Figure 4C). The loss of TLR7 processing was more marked when phagosomal fractions were examined: as shown in Figure 4D, DC1 pretreatment led to a complete loss of truncated TLR7 from THP-TLR7 phagosomes, which instead now contained full-length receptor. Similar results were obtained with DC2, another dicoumarol derivative that preferentially inhibits PC7 but has an additional effect on furin, PACE4, and PC5/6 (data not shown) (Komiyama et al., 2009).

LoVo cells do not produce functional furin (Takahashi et al., 1993; Zarkik et al., 1997) but express mRNA for *Pace4*, *Pc5/6*, and *Pc7* (data not shown). Like THP-TLR7 cells, LoVo cells expressing TLR7 (but not parental LoVo) were able to respond to R848 (another TLR7 agonist; Figure 5B and data not shown). Thus, our data suggest that other members of the furin-like PC family can substitute for furin in promoting TLR7 cleavage. To assess the role of PC5/6 and PC7 in TLR7 processing, we generated LoVo-TLR7 cells stably expressing the prosegments of *Pc5/6* (*ppPc5*) and/or *Pc7* (*ppPc7*), which act as specific inhibitors of the respective mature PC (Figure 5A; Fugère et al., 2002; Nour et al., 2003; Zhong et al., 1999). Expression of either *ppPc5* or

ppPc7 or (in particular) both prosegments led to a marked reduction in R848-induced IL-8 secretion (Figure 5B) and TLR7 processing (Figure 5C and data not shown). Thus, both proteases appear to process hTLR7. We then decreased *Pc5*, *Pc7*, or *Furin* expression in THP-TLR7 by using shRNA lentiviral particles targeting the respective proteases. *Furin* knockdown resulted in marked inhibition of TLR7 processing and of IL-8 production in response to R837 but not LPS (Figure 5D). This effect was seen with five different individual shRNA constructs targeting different regions of *Furin*, used separately or in combination (Figure 5D and data not shown). Consistent with these data, we were able to show furin in phagosomes of THP-1 cells (Figure S1E and data not shown). Knockdown of *Pc7*, but not *Pc5*, also inhibited TLR7 processing and R837 responsiveness to some degree (data not shown). We conclude that furin-like PCs in THP-1 and LoVo cells are necessary for processing of hTLR7.

Mutation of a Potential PC Recognition Site Reduces Human TLR7 Processing and Signaling

The hTLR7 protein sequence contains a prominent cluster of five putative PC cleavage sites between residues 467 and 480 within the flexible loop between LRR 14 and 15 (Figures 1C and S4A). To further examine the role of furin-like PCs in the processing of full-length TLR7, we removed all of the predicted furin-like PC recognition sites within the undefined region by replacing arginine 467 and arginine 473 with alanines (TLR7-mut; Figures 5E and S4A). Normal amounts of the TLR7-mut were expressed in PMA-differentiated THP-1 cells but the fraction of truncated protein was reduced (Figure 5F). This correlated with a lower response to R837 when compared to cells bearing wild-type TLR7 (Figure 5F), whereas the response to LPS was unaffected (Figure S4B). TLR7-mut was able to traffic to late endosomes and the extent of colocalization with the endosomal marker Lamp1 was similar for TLR7 and TLR7-mut (Figures S4C and S4D). We conclude that abrogation of putative furin-like PC cleavage sites in the flexible loop between LRRs 14 and 15 impairs processing of hTLR7 and decreases generation of a signaling-competent TLR7.

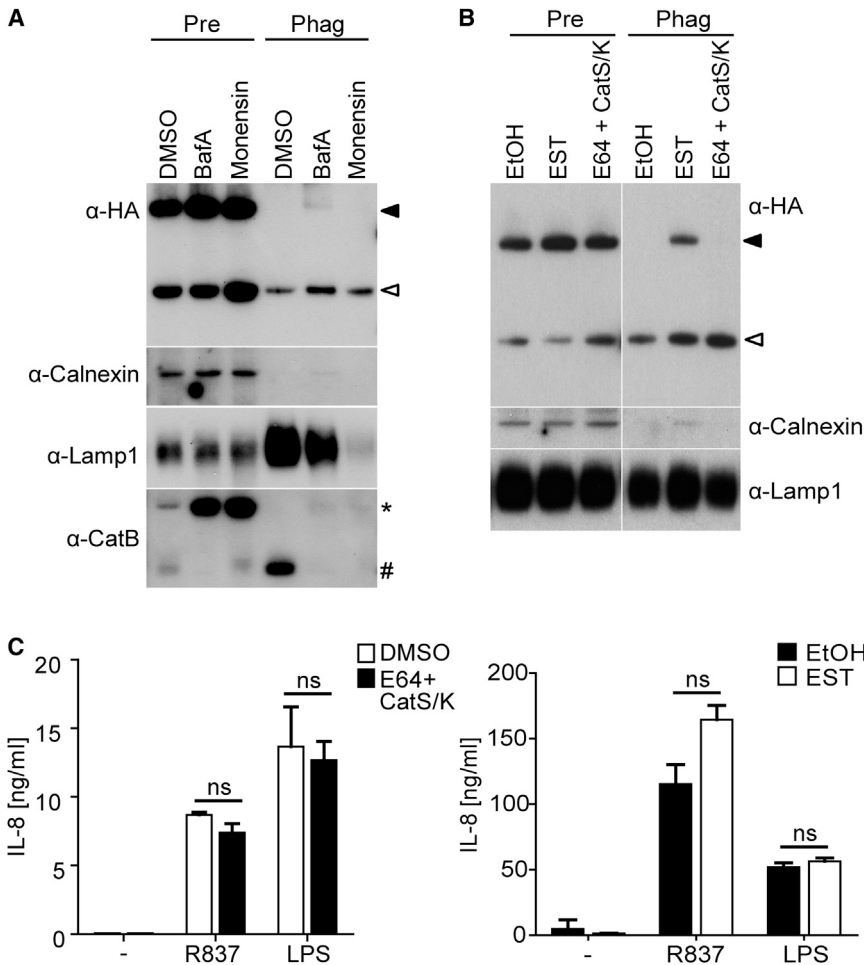


Figure 3. Inhibition of Acidification Does Not Affect the Generation of Truncated TLR7 and Its Accumulation in Phagosomes

(A) Immunoblot analysis of lysates of pregradient controls (Pre) or phagosome (Phag) fractions probed with antibodies with the indicated specificity. PMA-differentiated THP-TLR7 cells were treated with indicated inhibitors for 12 hr before feeding with latex beads in the presence of inhibitors and R837 for 6 hr.

(B) PMA-differentiated THP-TLR7 were treated with indicated inhibitors (E64 [20 μM], CatS [2 nM], CatK [1.5 μM], EST [20 μM]) or carrier (ethanol; EtOH) for 24 hr. Phagosomes were isolated and analyzed as described above.

Full-length and truncated TLR7 are shown by filled and open arrowheads, respectively. Asterisk (*) indicates immature pro-CatB and hatch sign (#) indicates mature CatB.

(C) PMA-differentiated THP-TLR7 cells were treated with the indicated inhibitors for 24 hr and then stimulated with R837 or LPS in the presence of inhibitors for another 24 hr. IL-8 accumulation in culture supernatants was measured by ELISA. Values are mean ± SD of triplicates. ns indicates nonsignificant versus control by Student's t test.

Representative of at least three independent experiments. See also Figure S2.

The C-Terminal Portion of Human TLR7 Is Signaling Competent

To verify the truncation site identified by site-directed mutagenesis and mass spectrometry analysis of the cleaved C-terminal fragment, we made HA-tagged hTLR7 C-terminal fragments (Cterm) of different lengths, starting after the different possible cleavage sites within the undefined region (Figure S5A). The construct CtermK starts at amino acid 481 and ends at position 1049 and therefore is similar to the C-terminal fragment of mTLR7, ranging from residue 480 to 1052, that is functionally active in cells overexpressing Unc93B1 (Maschalidi et al., 2012). We expressed all constructs in THP-1 cells (THP-Cterm) and carried out immunoblot analysis of PNGase F-treated cell lysates to eliminate the confounding effects of glycosylation (Figure S5B). The truncated version naturally found in cells expressing wild-type TLR7 ran at an apparent molecular weight between those of constructs CtermH to K (Figure S5B). Therefore, hTLR7 processing occurs at one of the potential furin-like PC recognition sites between amino acids 470 and 480.

Surprisingly, none of the C-terminal fragments rendered THP-1 cells responsive to R837 (Figure 6A and data not shown). This was not due to a lack of Unc93B1, because all transfectants expressed amounts of endogenous Unc93B1 (Figure S5C, top, and data not shown) comparable to those in cell lysates of primary

peripheral blood mononuclear cells (PBMCs), plasmacytoid dendritic cells (pDCs), and B cells (Figure S5C, bottom). Nevertheless, overexpression of C-terminally FLAG-tagged Unc93B1 (Figure S5D) did increase the IL-8 response of THP-CtermK cells to R837 by around 10-fold

(Figure 6A) and revealed the functional activity of the CtermK fragment, albeit at lower activity than for full-length TLR7 (Figure 6A).

An explanation for the reduced ability of the TLR7 C-terminal fragment to restore completely IL-8 response to R837 could be that the TLR7 N-terminal fragment is required to ensure efficient TLR7 trafficking into the endo-lysosomal compartment. Consistent with that notion, the CtermK fragment was not detected in phagosome fractions even though it could be easily detected in the pregradient controls (Figure S5E). We hypothesized that full-length TLR7 might be able to form a heterodimer with CtermK and escort the latter to the endocytic pathway. To test this hypothesis, THP-1 cells expressing the CtermK fragment and the full-length TLR7 were tested for their ability to respond to R837 in the presence or absence of DC1, which inhibits the biological activity of full-length TLR7 but should not affect that of the CtermK fragment. Consistent with this prediction, THP-1 cells coexpressing full-length TLR7 and the CtermK fragment produced IL-8 in response to R837 and were resistant to DC1 inhibition (Figure S5F). In contrast, as before, DC1-treated THP-1 cells expressing full-length TLR7 alone failed to respond to R837 stimulation (Figure S5F). Thus, expression of full-length TLR7 partially restores the activity of CtermK fragment in trans. Consistent with these findings, preliminary observations suggest

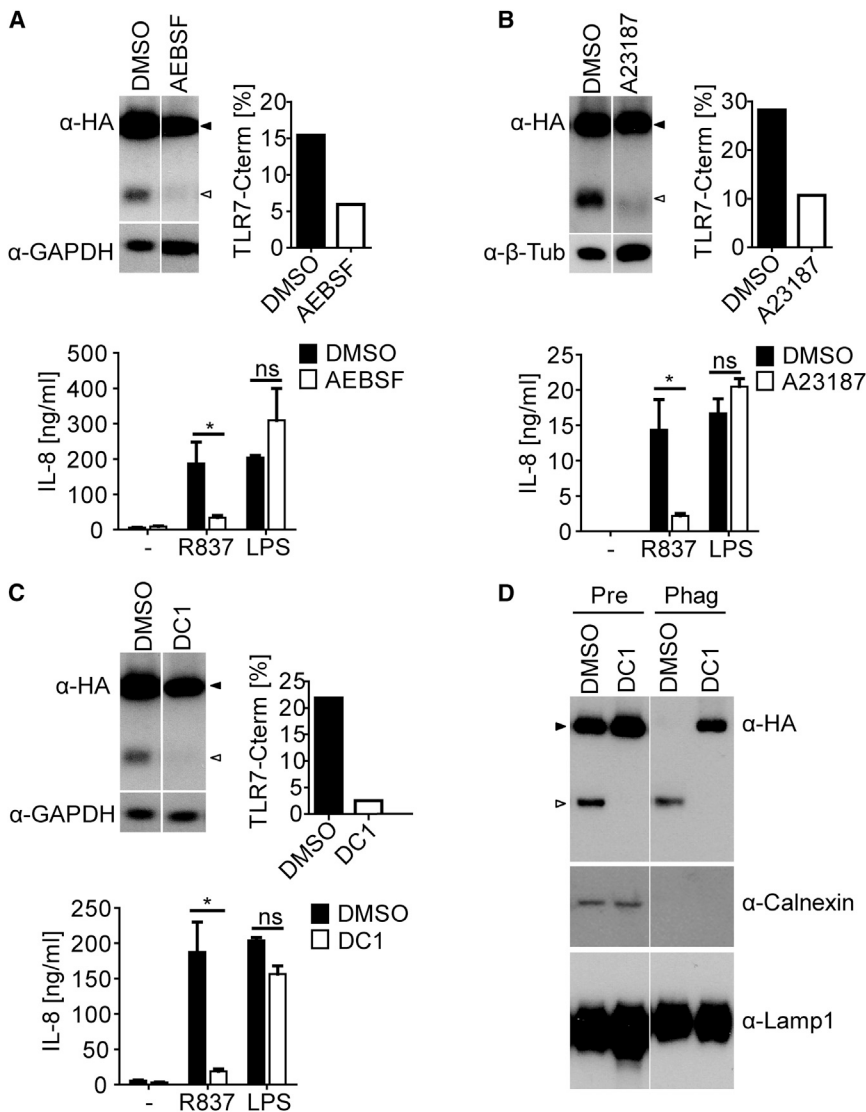


Figure 4. Calcium-Dependent Serine-Proteases Mediate TLR7 Processing

(A–C) Immunoblot analysis of cell lysates of PMA-differentiated THP-TLR7 treated with AEBSF (0.25 mM) (A), EDTA (0.5 mM) + A23187 (0.5 μM) (B), or DC1 (60 μM) (C) for 24 hr. Membranes were probed with the indicated antibodies. Band intensity is expressed as percentage of total TLR7. For cytokine analysis, cells were treated as described above and then stimulated with R837 or LPS in the presence of inhibitors for another 24 hr and IL-8 in culture supernatants was measured by ELISA. Values are mean ± SD of triplicates. ns indicates nonsignificant; *p < 0.05 versus control by Student's t test.

(D) Immunoblot analysis of lysates of pregradient controls (Pre) or phagosome fractions (Phag) probed with antibodies specific for the indicated proteins. PMA-differentiated THP-TLR7 cells were treated with inhibitors 24 hr prior to incubation with latex beads in the presence of R837.

Full-length and truncated TLR7 are shown by filled and open arrowheads, respectively. Representative of at least three independent experiments. See also Figure S3.

itive selection and cultured them with DC1 inhibitor or with solvent alone (DMSO). Unfortunately, the lack of antibodies suitable for biochemical detection of TLR7 prevented assessment of endogenous TLR7 cleavage in primary cells (data not shown). Nevertheless, across multiple experiments with cells from different donors, we noticed that pDCs preincubated with DC1 secreted markedly less IFN-α in response to R837 or heat-inactivated (56°C for 30 min) influenza virus (hiFlu), another TLR7 agonist (Diebold et al., 2004), when compared to DMSO-treated cells (Figure 7A). In addition,

that overexpression of the N-terminal hTLR7 fragment can also partially restore the functional activity of the C-terminal fragment (data not shown).

Finally, we extended these results by examining coupling to the downstream signaling adaptor MyD88. Confocal microscopy analysis showed that R837 stimulation enhanced colocalization of MyD88 with TLR7 in THP-TLR7 cells treated with DMSO, but not in cells treated with DC1 (Figures 6B and 6C). Because phagosomes purified from untreated THP-TLR7 cells contain only cleaved TLR7, whereas those purified from DC1-treated cells contain the full-length TLR7 (Figures 2D and 4D), these data indicate that MyD88 is specifically recruited in a ligand-dependent manner to endosomes containing the TLR7 C-terminal fragment but not full-length TLR7.

Furin-like PCs Are Required for TLR7 Responsiveness in Primary Human pDCs and B Cells

In humans, TLR7 expression is predominantly found on pDC and B cells. We purified human pDCs from peripheral blood by pos-

tion, cathepsin inhibitors had little effect on the response to hiFlu, even though they decreased the response to R837 (Figure S6A). We ruled out that lack of IFN-α was due to a toxic effect of the inhibitors by monitoring cell viability (data not shown) and metabolic activity (Figure S6B). As an additional source of cells expressing endogenous amounts of TLR7, we generated human IFN-DCs from blood monocytes by differentiation in the presence of IFN-α and GM-CSF (Mohty et al., 2003). Treatment of these cells with DC1, but not with DMSO, reduced their ability to produce IL-8 in response to R837 but not to LPS (Figure 7B), without affecting cell viability (data not shown). DC1 treatment of B cells isolated from peripheral blood decreased IL-8 secretion and upregulation of CD80 in response to R837 or hiFlu (Figure 7C). In contrast, the same response was not decreased by EST (data not shown). Next, we assessed the effect of furin-like PC inhibitors on the functional response to TLR9 agonists, because the lack of suitable antibodies prevented direct assessment of TLR9 cleavage. As shown in Figures 7D and 7E, DC1 markedly reduced CpG-induced activation of human pDCs

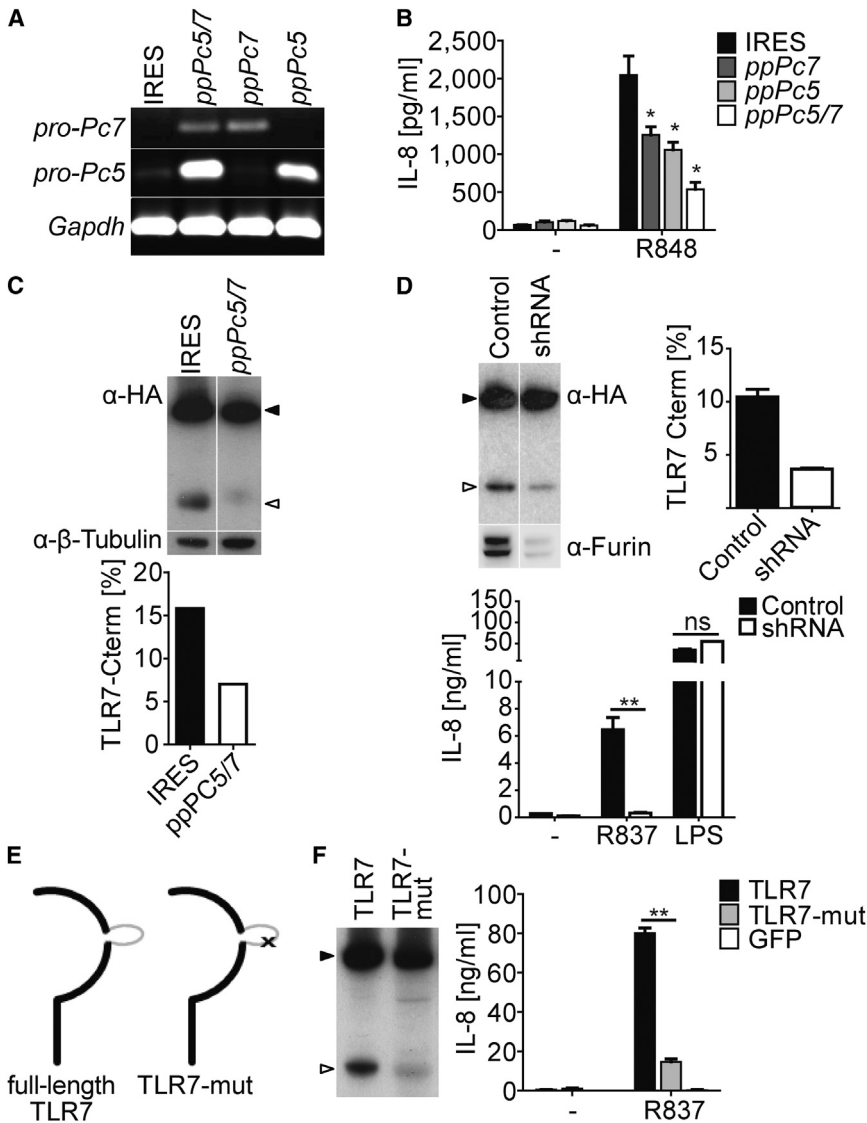


Figure 5. Furin, PC5/6, and PC7 Can Mediate TLR7 Processing

(A–C) LoVo-TLR7 cells stably expressing IRES control plasmid, or inhibitory preprosegments *ppPc7* or *ppPc5*, or *ppPc7* and *ppPc5* (*ppPc5/7*) together.

(A) Semiquantitative RT-PCR showing expression of preprosegments.

(B) IL-8 in supernatants of LoVo-TLR7 expressing the indicated preprosegments and stimulated for 24 hr with R848.

(C) Immunoblots of cell lysates of LoVo-TLR7 expressing *ppPc5* and *ppPc7* and stained for HA. Band intensity is expressed as percentage of total TLR7.

(D) Immunoblot of cell lysates of THP-TLR7 expressing shRNA against furin or nontarget controls stained for HA and furin (top). Band intensity is expressed as percentage of total TLR7 (top right). IL-8 in supernatant of the same cells stimulated for 24 hr with R837 (1 μg/ml) or LPS (0.1 μg/ml) (bottom).

(E) Schematic depiction of TLR7 and TLR7-mut. The flexible loop is depicted in gray. Mutation inserted within the flexible loop indicated by x.

(F) Cell lysates of PMA-differentiated THP-1 expressing indicated constructs were analyzed by staining with anti-HA. IL-8 accumulation in culture supernatants of indicated cell lines was monitored by ELISA after 24 hr of stimulation with R837 (10 μg/ml).

All IL-8 histograms show mean ± SD (n = 3). ns indicates nonsignificant; *p < 0.05; **p < 0.01 by Student's t test versus control. Full-length and truncated TLR7 are shown by filled and open arrowheads, respectively. Representative of either two (A) or at least three (B–D, F) independent experiments. See also Figure S4.

and B cells. In contrast, cathepsin inhibitors had no effect on pDCs in the same assay (Figure S6A, right). None of the inhibitors was toxic to the cells (Figure S6B).

PMA treatment enhanced expression of furin protein in pDCs, IFN-DCs, PBMCs, and B cells (Figure S6C). In pDCs furin was also upregulated by IFN-α treatment (Figure S6C) and in B cells by engagement of the B cell receptor, especially in combination with CD40L (Figure S6C). Furthermore, B cell receptor crosslinking, IFN-γ, and IFN-α all increased *Furin*, *Pc5*, and *Pc7* transcripts in B cells (Figure S6D). We conclude that furin-like PC activity is required to generate signaling-competent TLR7 in primary human cells and that expression of furin-like PCs is increased in those cells by exposure to proinflammatory and differentiation-inducing stimuli.

Finally, we assessed whether the role of furin-like PCs in TLR processing might extend to mouse. The aligned mouse and human TLR7 sequences showed (Figure 1C, bottom) furin-like PC recognition sites at the exact same positions. DC1 treatment reduced secretion of IL-12p40 by mouse macrophages in

strongly decreased responses to TLR7 and TLR9 agonists (data not shown). Thus, furin-like PCs play a role in the processing of TLRs across cell types and species, but other families of proteases also contribute to differing degrees.

DISCUSSION

The recent finding that endosomal TLRs require processing by low pH-dependent proteases has gained much attention as a mechanism for reinforcing self/nonself nucleic acid discrimination. However, most studies supporting this concept have been carried out with mTLR9 (Ewald et al., 2008; Park et al., 2008; Sepulveda et al., 2009) or, more recently, mTLR7 (Maschalidi et al., 2012) and have not been extended to human TLRs. In this study, we show that hTLR7 is proteolytically cleaved in different human immune and nonimmune cells and that receptor processing is required for functional activity. Notably, TLR7 cleavage generates a C-terminal fragment that selectively accumulates in compartments of the endocytic pathway and yet the

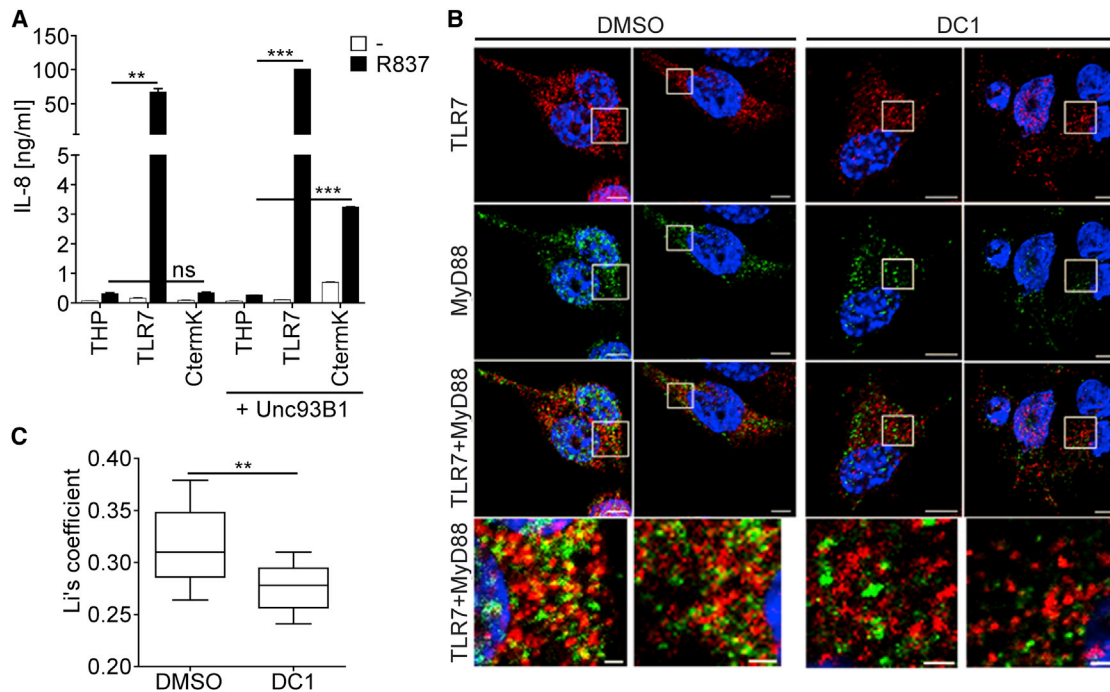


Figure 6. The Truncated Version of TLR7 Is Signaling Competent

(A) IL-8 secretion from THP-1 cells expressing the indicated constructs stimulated with R837 for 24 hr was measured by an ELISA. Values are mean \pm SD (n = 3). (B and C) THP-1 cells expressing HA-tagged TLR7 and FLAG-tagged MyD88 were PMA differentiated for 24 hr in the presence of DMSO or DC1 (70 μ m) and then stimulated for 3 hr with 5 μ g/ml R837.

(B) Cells were then fixed and stained with anti-HA (shown in red) and anti-FLAG (shown in green). Confocal pictures were taken. Scale bars represent 5 μ m (top three rows) and 1 μ m (bottom row).

(C) Li's coefficient of ≥ 10 cells per treatment was calculated to quantify the degree of colocalization of MyD88 and TLR7. Data obtained are represented as a box and whisker plot. Whiskers show minimum to maximum of all the data.

Stats versus control (Student's t test): **p < 0.01; ***p < 0.001. Representative of three independent experiments. See also Figure S5.

processing event is independent of the low pH found in those compartments, making the involvement of acidic proteases unlikely. Although our data do not fully rule out the involvement of cathepsins, in particular ones that might be active at neutral pH, we show that TLR7 processing requires calcium-dependent serine proteases of the furin-like PC family and identify an important site of furin-like PC cleavage within the loop between LRRs 14 and 15. These data extend to hTLR7 the processing paradigm first established for mTLRs, but unexpectedly reveal that it can occur independently of endosomal acidification and highlight furin-like PCs as an important family of proteases in the regulation of innate immune recognition.

Because acidification does not appear to be required for hTLR7 cleavage, processing can occur before the receptor reaches late endosomes, consistent with the fact that PCs can exert catalytic activity throughout the biosynthetic pathway. Thus, TLR7 cleavage might occur as early as the ER or Golgi before diversion of the receptor to the endocytic pathway (Lee et al., 2013). This early cleavage would ensure that a signaling-competent form of the receptor is already present in early endosomal compartments with low cathepsin content where TLR7 signaling has been reported to initiate (Honda et al., 2005a, 2005b; Sasai et al., 2010). However, our data also suggest that the N terminus of TLR7 helps direct the receptor to the appropriate endosomal compartment, in which case its premature loss would be detri-

mental. A recent study indicates that C- and N-terminal fragments of mTLR7 can remain linked to each other via disulfide bonds after cleavage (Kanno et al., 2013). Thus, early TLR7 cleavage by furin-like PCs need not preclude N-terminal-directed trafficking to endosomes in the absence of disulfide reduction. Although acidification was dispensable for cleavage, it remained necessary for cellular responses to TLR7 agonists. The question of why low pH is important for ligand recognition and signaling by endosomal TLRs remains unresolved (Rutz et al., 2004) but may be related to the protonation of specific histidine residues at acidic pHs within the ligand binding domain of TLRs (Govindaraj et al., 2011; Pirher et al., 2008). Another possibility is that low pH-dependent thiol reductases facilitate reduction of a putative disulfide link between the precleaved N- and C-terminal fragments and release of the signaling-competent TLR C-terminal fragment in the appropriate endosomal compartment.

Several of our findings were obtained with transfected cells overexpressing TLR7 in which some components of the TLR biosynthetic pathway might be limiting. This was not the fact for the more obvious player, Unc93B1 (Kim et al., 2008; Tabeta et al., 2006), because overexpression in THP-TLR7 enhanced the functional response to TLR7 agonists only slightly. Furthermore, we validated our results by using IFN- α differentiated monocyte-derived DCs and human blood pDCs and B cells.

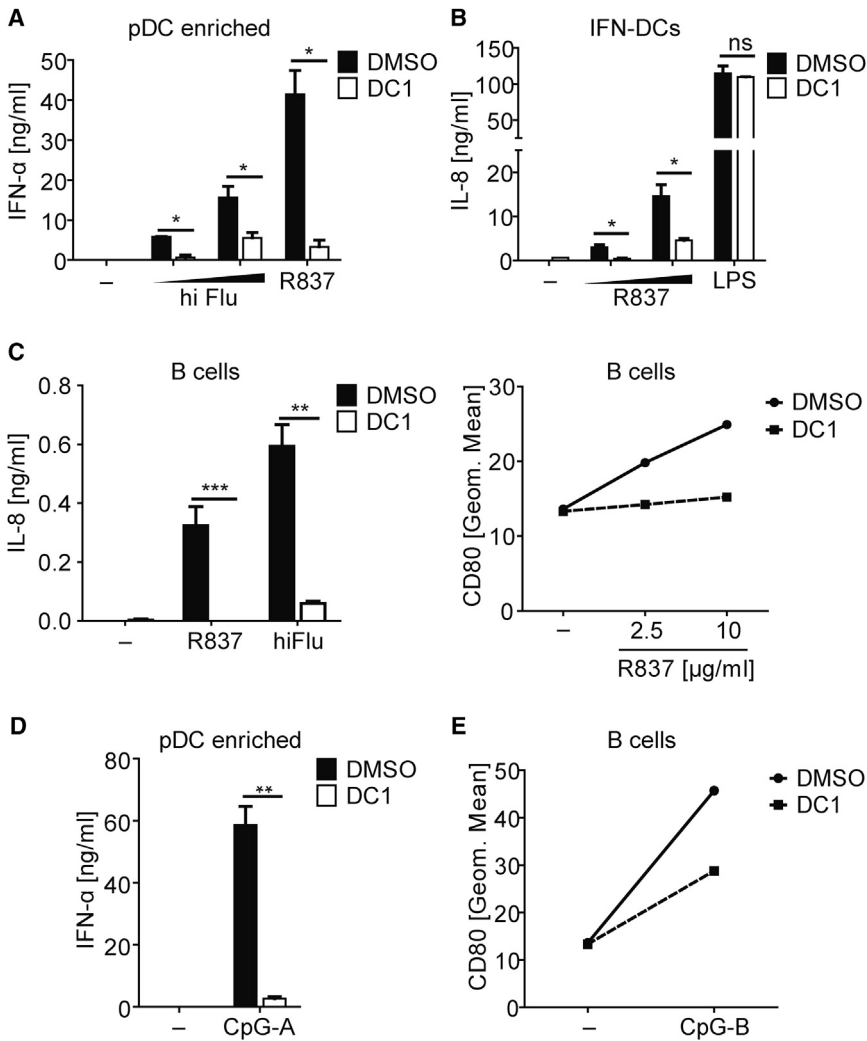


Figure 7. Pharmacological Inhibition of Furin-like PCs in pDCs and B Cells Reduces Responses to TLR7 and TLR9 Agonists

(A) Human pDC fractions were treated with DMSO or DC1 (70 μ M) for 24 hr and then stimulated with R837 (1 μ g/ml) or hiFlu (equivalent to MOIs of 0.5 or 1) overnight. IFN- α in supernatants was measured by ELISA. Histograms show mean \pm SD (n = 2).

(B) Human IFN-DCs were treated with DC1 (30 μ M) for 24 hr and then stimulated with R837 (2.5 or 5 μ g/ml) or LPS (0.5 μ g/ml) for 36 hr. Supernatants were harvested and IL-8 content was measured. Histograms show mean \pm SD (n = 3).

(C) Human blood B cells were treated with DMSO or DC1 (70 μ M) for 24 hr and then stimulated with R837 (10 μ g/ml) or hiFlu (equivalent to MOI of 1.6) for another 24 hr. IL-8 in supernatants was measured by ELISA (left) and upregulation of CD80 was analyzed by FACS (right). Values are mean \pm SD of triplicates.

(D) Human pDC fractions were treated with DMSO or DC1 (70 μ M) for 24 hr, and then stimulated with CpG-A (5 μ g/ml) overnight. IFN- α secretion was measured by ELISA. Values are mean \pm SD of duplicates.

(E) Human blood B cells were treated with DMSO or DC1 (70 μ M) for 24 hr and then stimulated with anti-Fab alone or with anti-Fab \pm CpG-B (5 μ M) for 24 hr. Upregulation of cell surface expressed CD80 was analyzed by flow cytometry.

ns indicates nonsignificant; *p < 0.05; **p < 0.01; ***p < 0.001 by Student's t test versus control. Representative of either at least three (A, B) or two (C–E) independent experiments. See also Figure S6.

Inhibition of furin-like PCs in these cells resulted in a reduced functional response to agonists of TLR7 and also of TLR9, arguing that our conclusions are generally applicable to TLR7 and, possibly, also to TLR9 regulation in primary human cells. Whether they are also applicable to the other nucleic-acid-sensing TLRs, such as TLR3 or TLR8, remains to be investigated. We also found that treatment of human primary B cells or THP-TLR7 cells with TLR7 agonists resulted in only a weak response, which could be markedly potentiated by pretreating with proinflammatory and differentiation stimuli. Those stimuli greatly increased the expression of furin-like PCs and enhanced TLR7 processing. Enhanced processing of TLR7 induced by inflammatory stimuli may therefore serve as a positive feedback mechanism during infection. In contrast, in noninflammatory situations, TLR7 processing might be limiting, contributing to preventing TLR7 activation by self-RNA reaching endosomal-lysosomal compartments.

Our preliminary studies suggest that furin-like PCs may also play a role in generating functional mTLR7 and mTLR9 in mouse macrophages. On the other hand, cathepsins and AEP clearly have a dominant role in processing of mTLRs (Ewald et al., 2008; Maschalidi et al., 2012; Park et al., 2008; Sepulveda

et al., 2009). Such results suggest that TLR7 cleavage may be differentially regulated in human versus mouse, as well as in different cell types. Differential protease dependence may also apply to different activation states of the same cell. Thus, it may be possible to envisage strategies that selectively inhibit TLR processing in specific cells by targeting different classes of proteases. In this regard, derivatives of dicoumarol have been extensively used in the clinic as anticoagulants and show high bioavailability and relatively low toxicity (Alexander, 1962). Our finding that furin-like PCs play an important role in TLR7 processing in human pDCs suggests that selective inhibition of PCs by dicoumarol derivatives could be useful as a therapeutic approach for TLR7- and pDC-driven immune pathologies, such as systemic lupus erythematosus.

EXPERIMENTAL PROCEDURES

More detailed description of reagents and experiments can be found in the Supplemental Experimental Procedures.

Generation of IFN-DCs, and pDC and B Cell Isolation

Human IFN-DCs were generated by in vitro differentiation of the CD14⁺ sub-population of PBMCs as described previously (Mohty et al., 2003). BDCA-4⁺ pDCs and CD19⁺ B cells were MACS sorted from leucocytes according to the manufacturer's instruction.

DNA Cloning, Site-Directed Mutagenesis, Lentiviral Transduction, and Gene Knockdown

hTlr7 tagged at the C terminus with HA was cloned into the lentiviral vector pHR-SIN-IRES-Em (Demaison et al., 2002). Double mutations were inserted with the quick QuikChange II XL Site-Directed Mutagenesis Kit (Stratagene) according to the manufacturer's conditions. MISSION shRNA lentiviral vectors were from Sigma-Aldrich. Lentiviral vectors encoding FLAG-tagged Unc93B1 or MyD88 were from GeneCopoeia. Cells transduced with lentiviruses were selected by FACS sorting or puromycin selection.

Cell Lysis and Quantitative Immunoblot Analysis

10^6 cells were lysed in 50 μ l 1% (v/v) Triton X-100 based lysis buffer. Where indicated, samples were digested with PNGase F (NEB). Proteins were separated by SDS-PAGE and standard immunoblot analysis was performed. To calculate the percentage of truncated TLR7 per lane, the intensity of the band of processed TLR7 was divided by the intensity of the band of total TLR7 (shorter + longer fragment).

Large-Scale Immunoprecipitation and Tandem Mass Spectrometry

Lysate of PMA-differentiated THP-TLR7 cells was precleared with mouse IgG-Agarose (Sigma) and immunoprecipitated with anti-HA-Agarose Clone HA-7 (Sigma). Eluted polypeptides were visualized by silver staining on SDS-PAGE, and then tandem mass spectrometry was performed on bands of interest.

IL-8, IFN- α , and mL12-p40 Assay

Cells were stimulated for 24 hr with indicated TLR agonists. Conditioned medium was collected and secretion of hIL-8, hIFN- α , or mL-12p40 was analyzed by enzyme-linked immunosorbent assay (ELISA).

Phagosome Isolation

Latex beads were fed to PMA-differentiated THP-1 cells, and cells were then disrupted by dounce homogenization. Latex-bead-containing phagosomes were isolated on a 60%–10% sucrose step gradient after ultracentrifugation. Phagosomes were lysed in lysis buffer, and proteins were separated by SDS-PAGE and visualized by immunoblot.

Transient Transfection and Antibiotic Selection

LoVo cells (70%–90% confluence) were transiently transfected by mixing either 1 or 2 μ g each of cDNAs of *ppPC5* (Nie et al., 2003) or *ppPC7* (Zhong et al., 1999) with 6 μ l FuGENE-6 as described by the manufacturer. After 12 hr, successfully transfected cells were selected by adding G418.

Confocal Microscopy

PMA-differentiated THP-1 cells were fixed, permeabilized with 0.5% Triton X-100, blocked, and then stained with primary followed by secondary antibodies. Images were taken with a confocal microscope and Li's coefficient was calculated to measure the extend of colocalization.

Semiquantitative RT-PCR

Semiquantitative RT-PCR for amplification of *ppPc5* and *ppPc7* and for *Gapdh* as housekeeping gene was performed as described in the [Supplemental Experimental Procedures](#).

Statistics

All values are represented as the mean \pm SD. An unpaired two-way Student's t test was performed to determine difference between the control and treated group. Significance was accepted at $p < 0.05$ versus control. * $p < 0.05$; ** $p < 0.01$; *** $p < 0.001$; **** $p < 0.0001$.

SUPPLEMENTAL INFORMATION

Supplemental Information includes Supplemental Experimental Procedures and six figures and can be found with this article online at <http://dx.doi.org/10.1016/j.immuni.2013.09.004>.

ACKNOWLEDGMENTS

The authors thank C. De Santo for generous practical and advisory input, S. Booth for practical and G. Napolitani for advisory input, and M. Johnson for critical reading and editing of the manuscript (all MRC Human Immunology Unit, University of Oxford, Oxford, UK). We thank G. Ball (Micron Oxford, Advanced Bioimaging Unit) for helping with the Fiji analysis and L. Chaperot as well as J. Plumas (Université Joseph Fourier, Grenoble, France) for experimental help. This work was supported by the Medical Research Council, UK, CRUK (Programme Grant # C399/A2291 to V.C. and LRI core support to C.R.S.), the Wellcome Trust (084923 to V.C.), DC-THERA, European Commission Sixth Framework Programme (Project Number 512074), the Harry Mahon Cancer Research Trust, UK, CIHR grant # MOP 44363, and a Canada Chair # 216684 (to N.G.S.). B.M.K. is supported by the Biomedical Research Centre (NIHR), Oxford, UK.

Received: January 23, 2012

Accepted: July 25, 2013

Published: October 17, 2013

REFERENCES

- Akira, S., Uematsu, S., and Takeuchi, O. (2006). Pathogen recognition and innate immunity. *Cell* 124, 783–801.
- Alexander, B. (1962). Anticoagulant therapy with coumarin congeners. Action and guidelines. *Am. J. Med.* 33, 679–691.
- Bell, J.K., Mullen, G.E.D., Leifer, C.A., Mazzoni, A., Davies, D.R., and Segal, D.M. (2003). Leucine-rich repeats and pathogen recognition in Toll-like receptors. *Trends Immunol.* 24, 528–533.
- Blasius, A.L., and Beutler, B. (2010). Intracellular toll-like receptors. *Immunity* 32, 305–315.
- Brinkmann, M.M., Spooner, E., Hoebe, K., Beutler, B., Ploegh, H.L., and Kim, Y.-M. (2007). The interaction between the ER membrane protein UNC93B and TLR3, 7, and 9 is crucial for TLR signaling. *J. Cell Biol.* 177, 265–275.
- Decroly, E., Wouters, S., Di Bello, C., Lazure, C., Ruyschaert, J.M., and Seidah, N.G. (1996). Identification of the paired basic convertases implicated in HIV gp160 processing based on in vitro assays and expression in CD4(+) cell lines. *J. Biol. Chem.* 271, 30442–30450.
- Demaison, C., Parsley, K., Brouns, G., Scherr, M., Battmer, K., Kinnon, C., Grez, M., and Thrasher, A.J. (2002). High-level transduction and gene expression in hematopoietic repopulating cells using a human immunodeficiency virus type 1-based lentiviral vector containing an internal spleen focus forming virus promoter. *Hum. Gene Ther.* 13, 803–813.
- Diebold, S.S., Kaisho, T., Hemmi, H., Akira, S., and Reis e Sousa, C. (2004). Innate antiviral responses by means of TLR7-mediated recognition of single-stranded RNA. *Science* 303, 1529–1531.
- Diebold, S.S., Massacrier, C., Akira, S., Paturel, C., Morel, Y., and Reis e Sousa, C. (2006). Nucleic acid agonists for Toll-like receptor 7 are defined by the presence of uridine ribonucleotides. *Eur. J. Immunol.* 36, 3256–3267.
- Ewald, S.E., Lee, B.L., Lau, L., Wickliffe, K.E., Shi, G.P., Chapman, H.A., and Barton, G.M. (2008). The ectodomain of Toll-like receptor 9 is cleaved to generate a functional receptor. *Nature* 456, 658–662.
- Ewald, S.E., Engel, A., Lee, J., Wang, M., Bogyo, M., and Barton, G.M. (2011). Nucleic acid recognition by Toll-like receptors is coupled to stepwise processing by cathepsins and asparagine endopeptidase. *J. Exp. Med.* 208, 643–651.
- Fugère, M., Limperis, P.C., Beaulieu-Audy, V., Gagnon, F., Lavigne, P., Klarskov, K., Leduc, R., and Day, R. (2002). Inhibitory potency and specificity of subtilase-like pro-protein convertase (SPC) prodomains. *J. Biol. Chem.* 277, 7648–7656.
- Govindaraj, R.G., Manavalan, B., Basith, S., and Choi, S. (2011). Comparative analysis of species-specific ligand recognition in Toll-like receptor 8 signaling: a hypothesis. *PLoS ONE* 6, e25118.
- Hallenberger, S., Bosch, V., Angliker, H., Shaw, E., Klenk, H.D., and Garten, W. (1992). Inhibition of furin-mediated cleavage activation of HIV-1 glycoprotein gp160. *Nature* 360, 358–361.

- Heil, F., Hemmi, H., Hochrein, H., Ampenberger, F., Kirschning, C., Akira, S., Lipford, G., Wagner, H., and Bauer, S. (2004). Species-specific recognition of single-stranded RNA via toll-like receptor 7 and 8. *Science* 303, 1526–1529.
- Honda, K., Ohba, Y., Yanai, H., Negishi, H., Mizutani, T., Takaoka, A., Taya, C., and Taniguchi, T. (2005a). Spatiotemporal regulation of MyD88-IRF-7 signaling for robust type-I interferon induction. *Nature* 434, 1035–1040.
- Honda, K., Yanai, H., Negishi, H., Asagiri, M., Sato, M., Mizutani, T., Shimada, N., Ohba, Y., Takaoka, A., Yoshida, N., and Taniguchi, T. (2005b). IRF-7 is the master regulator of type-I interferon-dependent immune responses. *Nature* 434, 772–777.
- Kagan, J.C. (2012). Signaling organelles of the innate immune system. *Cell* 151, 1168–1178.
- Kanno, A., Yamamoto, C., Onji, M., Fukui, R., Saitoh, S., Motoi, Y., Shibata, T., Matsumoto, F., Muta, T., and Miyake, K. (2013). Essential role for Toll-like receptor 7 (TLR7)-unique cysteines in an intramolecular disulfide bond, proteolytic cleavage and RNA sensing. *Int. Immunol.* 25, 413–422.
- Kim, Y.M., Brinkmann, M.M., Paquet, M.E., and Ploegh, H.L. (2008). UNC93B1 delivers nucleotide-sensing toll-like receptors to endolysosomes. *Nature* 452, 234–238.
- Komiyama, T., Coppola, J.M., Larsen, M.J., van Dort, M.E., Ross, B.D., Day, R., Rehemtulla, A., and Fuller, R.S. (2009). Inhibition of furin/proprotein convertase-catalyzed surface and intracellular processing by small molecules. *J. Biol. Chem.* 284, 15729–15738.
- Krug, A. (2008). Nucleic acid recognition receptors in autoimmunity. *Handb. Exp. Pharmacol.* 183, 129–151.
- Leadbetter, E.A., Rifkin, I.R., Hohlbaum, A.M., Beaudette, B.C., Shlomchik, M.J., and Marshak-Rothstein, A. (2002). Chromatin-IgG complexes activate B cells by dual engagement of IgM and Toll-like receptors. *Nature* 416, 603–607.
- Lee, B.L., Moon, J.E., Shu, J.H., Yuan, L., Newman, Z.R., Schekman, R., and Barton, G.M. (2013). UNC93B1 mediates differential trafficking of endosomal TLRs. *Elife* 2, e00291.
- Logeat, F., Bessia, C., Brou, C., LeBail, O., Jarrault, S., Seidah, N.G., and Israël, A. (1998). The Notch1 receptor is cleaved constitutively by a furin-like convertase. *Proc. Natl. Acad. Sci. USA* 95, 8108–8112.
- Malfait, A.-M., Arner, E.C., Song, R.-H., Alston, J.T., Markosyan, S., Staten, N., Yang, Z., Griggs, D.W., and Tortorella, M.D. (2008). Proprotein convertase activation of aggrecanases in cartilage in situ. *Arch. Biochem. Biophys.* 478, 43–51.
- Maschalidi, S., Hässler, S., Blanc, F., Sepulveda, F.E., Tohme, M., Chignard, M., van Endert, P., Si-Tahar, M., Descamps, D., and Manoury, B. (2012). Asparagine endopeptidase controls anti-influenza virus immune responses through TLR7 activation. *PLoS Pathog.* 8, e1002841.
- Mohty, M., Vialle-Castellano, A., Nunes, J.A., Isnardon, D., Olive, D., and Gaugler, B. (2003). IFN- α skews monocyte differentiation into Toll-like receptor 7-expressing dendritic cells with potent functional activities. *J. Immunol.* 171, 3385–3393.
- Molloy, S.S., Bresnahan, P.A., Leppla, S.H., Klimpel, K.R., and Thomas, G. (1992). Human furin is a calcium-dependent serine endoprotease that recognizes the sequence Arg-X-X-Arg and efficiently cleaves anthrax toxin protective antigen. *J. Biol. Chem.* 267, 16396–16402.
- Nie, G.Y., Li, Y., Minoura, H., Findlay, J.K., and Salamonsen, L.A. (2003). Specific and transient up-regulation of proprotein convertase 6 at the site of embryo implantation and identification of a unique transcript in mouse uterus during early pregnancy. *Biol. Reprod.* 68, 439–447.
- Nour, N., Basak, A., Chrétien, M., and Seidah, N.G. (2003). Structure-function analysis of the prosegment of the proprotein convertase PC5A. *J. Biol. Chem.* 278, 2886–2895.
- Park, B., Brinkmann, M.M., Spooner, E., Lee, C.C., Kim, Y.-M., and Ploegh, H.L. (2008). Proteolytic cleavage in an endolysosomal compartment is required for activation of Toll-like receptor 9. *Nat. Immunol.* 9, 1407–1414.
- Pirher, N., Ivicak, K., Pohar, J., Bencina, M., and Jerala, R. (2008). A second binding site for double-stranded RNA in TLR3 and consequences for interferon activation. *Nat. Struct. Mol. Biol.* 15, 761–763.
- Rousselet, E., Benjannet, S., Hamelin, J., Canuel, M., and Seidah, N.G. (2011a). The proprotein convertase PC7: unique zymogen activation and trafficking pathways. *J. Biol. Chem.* 286, 2728–2738.
- Rousselet, E., Benjannet, S., Marcinkiewicz, E., Asselin, M.C., Lazure, C., and Seidah, N.G. (2011b). Proprotein convertase PC7 enhances the activation of the EGF receptor pathway through processing of the EGF precursor. *J. Biol. Chem.* 286, 9185–9195.
- Rutz, M., Metzger, J., Gellert, T., Luppa, P., Lipford, G.B., Wagner, H., and Bauer, S. (2004). Toll-like receptor 9 binds single-stranded CpG-DNA in a sequence- and pH-dependent manner. *Eur. J. Immunol.* 34, 2541–2550.
- Salvas, A., Benjannet, S., Reudelhuber, T.L., Chrétien, M., and Seidah, N.G. (2005). Evidence for proprotein convertase activity in the endoplasmic reticulum/early Golgi. *FEBS Lett.* 579, 5621–5625.
- Sasai, M., Linehan, M.M., and Iwasaki, A. (2010). Bifurcation of Toll-like receptor 9 signaling by adaptor protein 3. *Science* 329, 1530–1534.
- Seidah, N.G., Mayer, G., Zaid, A., Rousselet, E., Nassoury, N., Poirier, S., Essalmani, R., and Prat, A. (2008). The activation and physiological functions of the proprotein convertases. *Int. J. Biochem. Cell Biol.* 40, 1111–1125.
- Sepulveda, F.E., Maschalidi, S., Colisson, R., Heslop, L., Ghirelli, C., Sakka, E., Lennon-Duménil, A.M., Amigorena, S., Cabanie, L., and Manoury, B. (2009). Critical role for asparagine endopeptidase in endocytic Toll-like receptor signaling in dendritic cells. *Immunity* 31, 737–748.
- Shlomchik, M.J. (2009). Activating systemic autoimmunity: B's, T's, and tolls. *Curr. Opin. Immunol.* 21, 626–633.
- Tabeta, K., Hoebe, K., Janssen, E.M., Du, X., Georgel, P., Crozat, K., Mudd, S., Mann, N., Sovath, S., Goode, J., et al. (2006). The Unc93b1 mutation 3d disrupts exogenous antigen presentation and signaling via Toll-like receptors 3, 7 and 9. *Nat. Immunol.* 7, 156–164.
- Takahashi, S., Kasai, K., Hatsuzawa, K., Kitamura, N., Misumi, Y., Ikehara, Y., Murakami, K., and Nakayama, K. (1993). A mutation of furin causes the lack of precursor-processing activity in human colon carcinoma LoVo cells. *Biochem. Biophys. Res. Commun.* 195, 1019–1026.
- Zarkik, S., Decroly, E., Wattiez, R., Seidah, N.G., Burny, A., and Ruyschaert, J.M. (1997). Comparative processing of bovine leukemia virus envelope glycoprotein gp72 by subtilisin/kexin-like mammalian convertases. *FEBS Lett.* 406, 205–210.
- Zhong, M., Munzer, J.S., Basak, A., Benjannet, S., Mowla, S.J., Decroly, E., Chrétien, M., and Seidah, N.G. (1999). The prosegments of furin and PC7 as potent inhibitors of proprotein convertases. In vitro and ex vivo assessment of their efficacy and selectivity. *J. Biol. Chem.* 274, 33913–33920.